

Product Performance

Deformation of reinforced polymer bearing elements on full-scale compressive strength and creep tests under yielding conditions

P. Samyn^{a,*}, L. Van Schepdael^b, J.S. Leendertz^c,
W. Van Paepegem^a, P. De Baets^a, J. Degrieck^a

^a *Laboratory Soete, Department Mechanical Construction and Production, Ghent University, St Pietersnieuwstraat 41, B-9000 Gent, Belgium*

^b *SOLICO B.V., Solutions in Composites, Everdenberg 97, NL-4902 TT Oosterhout, The Netherlands*

^c *Ministry of Transport, Public Works and Water Management, Directorate-General, Herman Gorterhove 4, NL-2700 AB Zoetermeer, The Netherlands*

Received 1 September 2005; accepted 14 October 2005

Abstract

Ultra high molecular weight polyethylene (UHMWPE) reinforced with a carbon fibre/epoxy ring (hybrid polymer pad) is used as bearing elements in a ball-joint for rotation of a storm surge barrier, requiring high strength and dimensional stability. The concave bearing surfaces contain 500 pads with diameter 250 mm incorporated in machined holes. As they are used as functional parts, high deformation will cause failure due to loss of clearance between the convex and concave surfaces. The applicability of general models for deformation of polymers to present structural design is limited, as they are based on material models and the effect of reinforcements should be verified. For optimisation and reliability, the present study focuses on a component test with a simulation of the real contact situation as closely as possible. From local analysis of the bearing elements, each polymer pad is loaded at 150 MPa, well above the polyethylene yield strength of 21 MPa. Full-scale experimental tests show two important details for stable deformation and life-time functionality, i.e. the clearance between the hybrid UHMWPE pad and its sample holder and the cold flow of a polymer lip over the carbon fibre ring for avoiding contact between the reinforcing ring and the convex counterface. Therefore, different geometries are evaluated with a total deformation of 10% during compression and 0.5% during subsequent creep. After recovery, a permanent deformation less than 1% is measured. For cold flow of the polymer lip, both the lip diameter and lip thickness should be controlled. Finally, a loading capacity of 400 MPa is determined for a hybrid UHMWPE pad.

© 2005 Elsevier Ltd. All rights reserved.

Keywords: Full-scale test; Hybrid UHMWPE pad; Creep, Strength

1. Introduction

Polymers have been favourably introduced as sliding materials in offshore structures for over ten years because of good wear resistance. Mainly under high loads, surface plastification contributes to low friction,

which is favourable for a reduction in dissipated sliding energy. The tribological characteristics of polymers above yield strength were recently demonstrated in Ref. [1], performing better than grease lubricants or self-lubricating coatings, which are easily removed and lead to catastrophic failure. Practical applicability of polymers is, however, restricted to relatively low loads compared to metallic parts. Under high loads, creep and deformation should be controlled and the design of polymer bearings not only deals with dynamic properties, but also with its long-term static loading capacity

* Corresponding author. Tel.: +32 9 264 33 08; fax: +32 9 264 32 95.

E-mail address: pieter.samyn@ugent.be (P. Samyn).

Nomenclature

| | | | |
|----------|---------------------------|-----|----------------------------|
| δ | vertical indentation (mm) | X | polymer lip thickness (mm) |
| D | polymer lip diameter (mm) | | |

(strength and dimensional stability). Sliding elements are mainly designed as functional components and high deformation after creep and recovery results in a change of clearance with implications for the operating construction, possibly leading to failure due to overload rather than wear. Reinforcing systems for polymer materials, consisting of high-strength materials such as metals or composites to carry the implied loads and minimise creep, should therefore be considered.

It is clear that the behaviour of such hybrid systems is difficult to predict as many parameters play an important role. Information on the long-term deformation and strength is normally extrapolated from short-term test data, obtained from accelerated testing conditions such as higher temperature, stress and humidity. However, the accuracy of a creep prediction depends on the accuracy of the available models as well as on its validity in the extrapolation range of stresses, which are presently well above the material's yield strength. Other models require input of mechanical parameters (e.g. modulus of elasticity, stiffness, etc), while a bulk modulus should be determined for reinforced structures. As the latter strongly depends on the test layout and is scarcely reported in literature, it should be experimentally measured from a test set-up that simulates the real working environment as closely as possible. For reliable polymer design, a constitutive model should be available under different loading conditions, such as uniaxial or multi-axial monotonic and cyclic loading. Different available models are given by Colak et al. [2]. Modifications of general creep models, regarding the activation theory and transitions in number of microscopic flow units depending on the strain increment, are discussed by Raghavan and Meshii [3]. Most creep and deformation models [4–6] are, however, based on 'material-tests' while for the present application a 'component-test' is required for simulating the boundary conditions of the steel structure and composite reinforcement. Moreover, full-scale tests are needed for quality control of the material production process.

Carbon fibre/epoxy ring reinforced UHMWPE discs (hybrid UHMPWE pad) are used as sliding material in the Maeslant storm surge barrier near Rotterdam (NL). For rotation of two retaining walls from the banks into

the river during a storm, the steel structure is connected to a steel ball (convex) with a diameter of 10 m and a weight of 680 ton. The ball surface is protected against corrosion through application of a Zn-phosphate primer coating and rests in concave chairs. Five hundred polymer pads are incorporated in holes machined into the concave structures, bearing a total load of 350×10^6 N during operation. The hole geometries were derived from a global finite element analysis, resulting in a diameter of 250 mm and a depth of 32 mm. The polymer pads have a nominal diameter of 249.50 mm and a thickness of 40 mm, giving a free surface of 8 mm above the steel surface. The final concept was implemented and proven in-the-field by the Nederlandse Rijkswaterstaat.

The present paper is part of an international test program performed at Ghent University (Laboratory Soete) and Solico (Solutions in Composites) for design of the polymer pads, only considering the behaviour of a local hybrid UHMWPE pad. The friction and wear characteristics of the UHMWPE and Zn-primer coating were previously tested on a large-scale tribotester [7]. Validation of compressive strength, creep and irreversible deformation is now evaluated by means of full-scale loading tests. The contact pressure on each bearing element is calculated from finite element analysis, resulting in a maximum of 150 MPa under working conditions. Generally, Collier et al. [8] cited a 21 MPa tensile yield strength for polyethylene, while Buechel et al. [9] used a 32 MPa compressive yield strength and a damage threshold of 5 MPa. Bartel et al. [10] used a 12.7 MPa yield strength, while Hayes et al. [11] used 14–15 MPa. Nevertheless, Bristol et al. [12] also found that the contact stresses in several non-conforming designs are much higher than the tensile yield strength and rise towards the 30–40 MPa range, with 80% of the total contact area typically overloaded above the 10 MPa damage threshold/fatigue strength. Also, Hood et al. [13] found that contact stresses on UHMWPE may locally exceed the yield strength. For stable deformation, it is presently important to consider the influence of machining tolerances on the pad dimensions, as any excess local deformation possibly causes overload on a neighbouring polymer disc and construction failure.

2. Experimental test set-up

2.1. Test material

Non-regenerated GUR 4120 [14] is used as compression moulded UHMWPE. Creep according to ISO 899 under various tensile stresses at 23 °C over a period of 8 weeks is given in Fig. 1(a), serving as a first approximation for the values to be expected under compressive stress. The yielding, plastic flow and fracture behaviour under low contact stresses (< 30 MPa) was tested on small-scale specimens by Kurtz et al. [15], concluding that the true stress strain behaviour of UHMWPE in tension and compression is only identical up to 0.12 true strain. Also, creep tests under uniaxial stress have limited applicability to the multi-axial or hydrostatic stress state. When the stress is removed from the test specimen, partial recovery takes place (Fig. 1(b)). Only creep at room temperature is presently considered. Although it was calculated from frictional heating [7] that the flash temperature attains 125 °C, this only occurs over $\pm 10 \mu\text{m}$ surface depth and does not influence the polymer bulk properties (maximum bulk temperature 40–60 °C).

A reinforcing composite ring is made of uni-directional high-modulus carbon fibre Toray T700 12K (1.8 g/cm³) and epoxy resin (1.09 g/cm³) that is hoop wound and machined. Fibre percentages are between 58 and 63% with a porosity content <2.5%. The curing times and temperatures were strictly controlled at 16 h at room temperature, 8–10 h at 60 °C and 8–10 h at 120 °C (15 C/h). Finally, the carbon fibre/epoxy rings are fitted on the UHMWPE pad at –20 °C.

Two types of hybrid pad geometries are included in present design tests. The pre-design Type I pad

(Fig. 2(a)) has a shoulder containing the carbon composite ring and is called a hybrid pad with ‘free’ carbon reinforcing ring. The polymer sliding surface is 2 mm above the ring and has a nominal diameter of 210 mm on top and 249.50 mm at the bottom. Contact between the carbon ring and the Zn-phosphate primer coated convex counterface under sliding leads to unacceptable abrasive wear. Therefore, Type II pads (Fig. 2(b)) contain a polymer lip covering the carbon composite ring and is called a hybrid pad with ‘embedded’ carbon reinforcing ring. Different lip geometries with variable diameter D and thickness X are applied, affecting the deformation stability. The top section contains the UHMWPE contact surface with a triangular pattern (side 13.5 mm) of circular undulations (\varnothing 4 mm) to hold an eventual lubricant. The rubber ring near the bottom (diameter 5.7 mm) ensures axial fixation of the hybrid UHMWPE pad into its holder. Present static loading tests include pad geometries with nominal diameter 249.50 mm (scale 1/1) and nominal diameter 175.00 mm (scale 1/1.43).

2.2. Full-scale static loading and creep tests

The local contact situation for a hybrid UHMWPE pad is simulated by the test setup in Fig. 3(a), using a vertical AMSLER 10,000 kN hydraulic press. The pad is mounted in the sample holder (Fig. 3(b)), consisting of a backing plate with a machined ring (\varnothing 250.00 mm \times 32 mm depth) and a curved counterface with radius 5000 mm. The hybrid pads have a free neck of 8 mm out of the holder and the steel counterface with roughness $R_a = 3.2 \mu\text{m}$ is coated with a Zn-phosphate primer. The sample holder is horizontally centred on a table (2) under the hydraulic press and loaded by a vertical jack (3) pushing the holder and its pad against

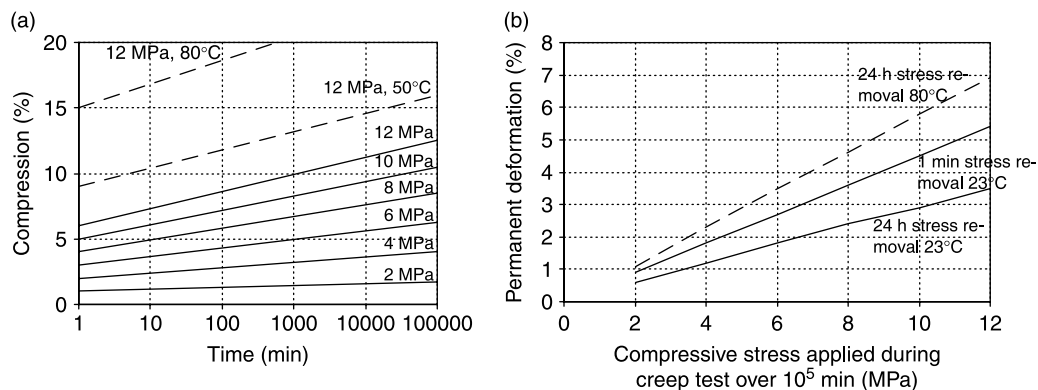


Fig. 1. Standard creep data for GUR 4120 according to ISO 899 [16,17], (a) creep under low contact pressures 2–12 MPa, (b) recovery measured over 24 h after loading at different compressive stresses.

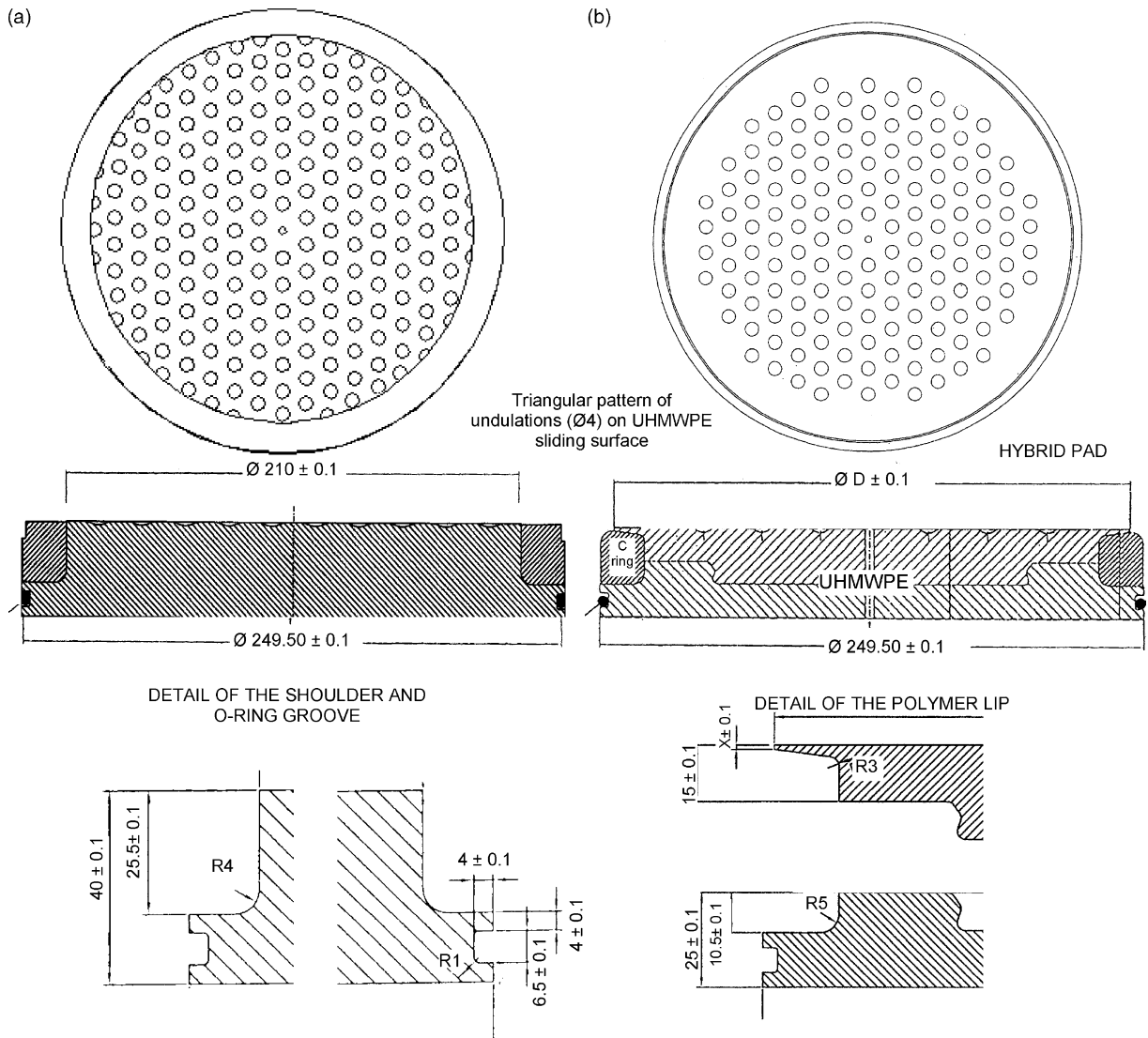


Fig. 2. Test specimens: Hybrid UHMWPE pads, (a) Type I pad with free carbon/fibre epoxy reinforcing ring, (b) Type II pad with embedded carbon fibre/epoxy reinforcing ring and different designs of lip diameter D (244, 239, 237, 236 mm) and lip thickness X (1.1, 1.5, 1.6 mm).

the fixed upper frame plate (1). The applied normal load is stepwise increased at 30 MPa/min towards 150 MPa, measuring the vertical indentation of the polymer pad as the vertical displacement of the upper counterplate relative to the table, by means of four displacement transducers. Test conditions are chosen in accordance with FEM calculations on the ball-joint with intermediate contact pressures of 30, 60, 90 and 120 MPa remaining constant for 2 h (short-time test) and the highest contact pressure (150 MPa) applied for 24 h (long-time creep test). The recovery was measured for 12 h after removal of the normal load (Fig. 3(c)). Finally, an overload (180 or 400 MPa for 5 min) is applied. The life-term stability of the pads is evaluated

by a 7 day creep test under 75 MPa, simulating the out-of-service period of the ball-joint. Deformations below are given in mm, related to the practical implementation for change in clearances between convex and concave ball-joint surfaces.

3. Test results: characterisation of local pad deformation

3.1. Stress-strain characteristics under compressive stress

The stress-strain curves of a Type I and Type II hybrid pad with different initial pad diameters under

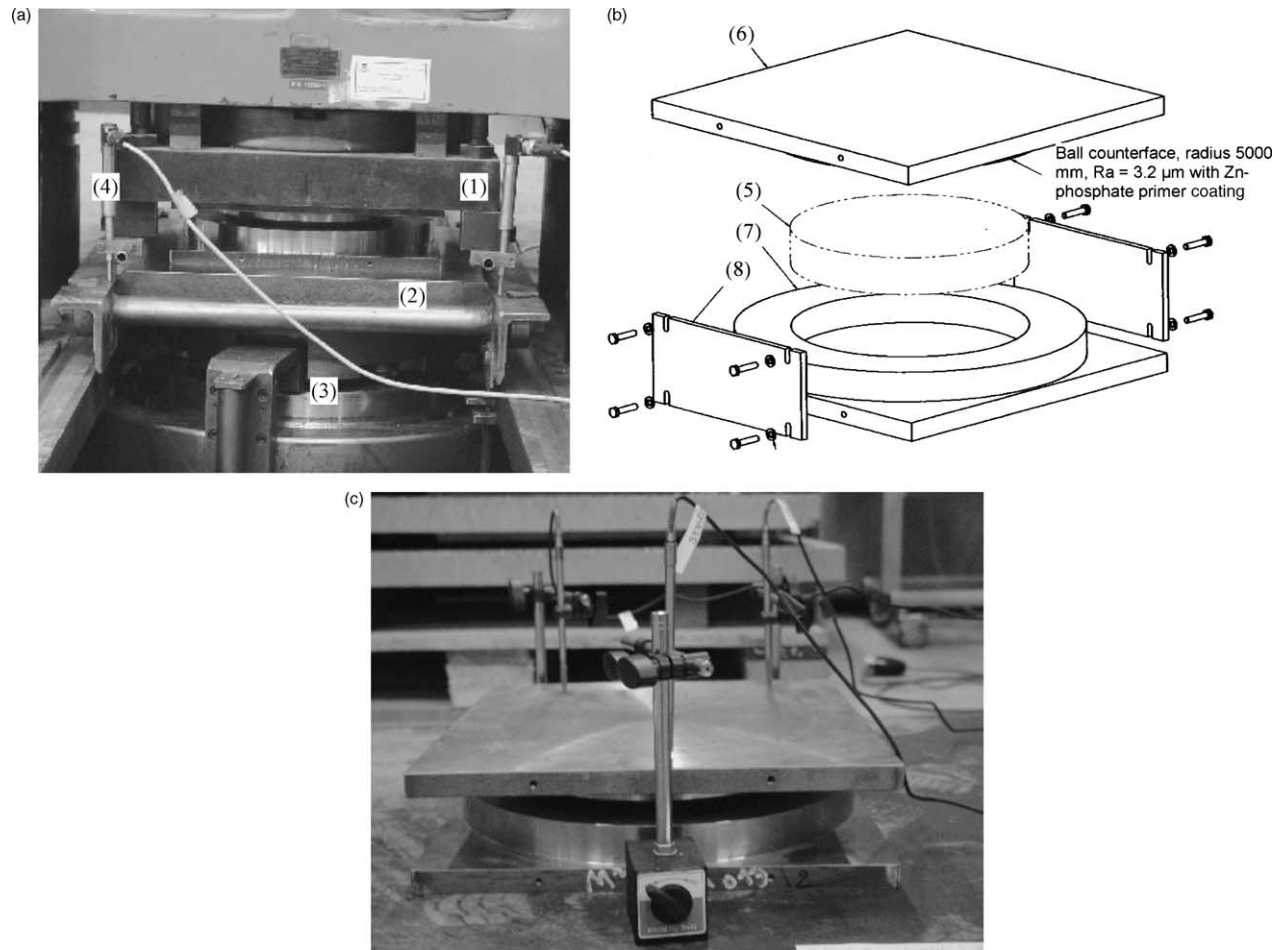


Fig. 3. Full-scale static loading test, (a) vertical hydraulic press 10,000 kN, (b) sample holder with ball counterface plate, (c) stress-free set-up during recovery measurements: (1) fixed upper plate of press, (2) moveable table, (3) vertical hydraulic piston, (4) displacement transducers, (5) hybrid UHMWPE pad, (6) counterplate, (7) sample holder or steel ring, (8) clamps used for mounting and positioning counterplate (opened during test).

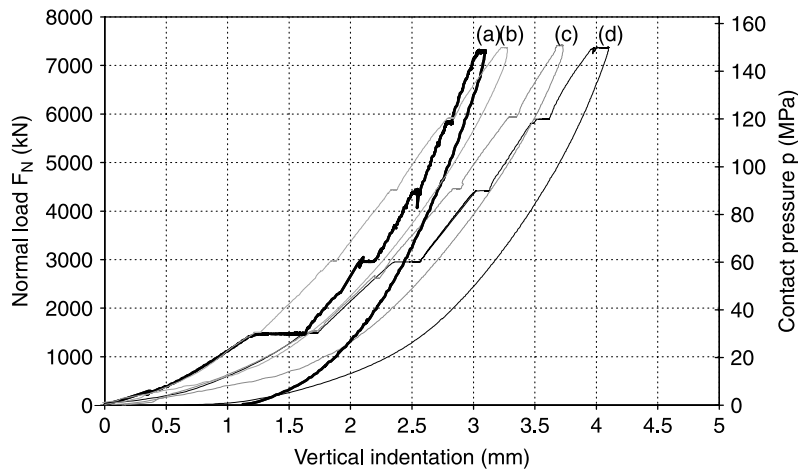


Fig. 4. Representative stress–strain characteristics for hybrid UHMWPE pads under uniaxial compression test, (a) Type I pad, (b–d) Type II pads with different initial pad diameter.

stepwise loading to working conditions of 150 MPa are shown in Fig. 4. The Type I pad shows lower total deformation than Type II pads. For different pad pad geometries, the stiffness k (N/mm^2) at high loads (between 120 and 150 MPa) and maximum indentation at 150 MPa is summarized in Table 1. The difference between δ_{120} , $\delta_{120(2\text{ h})}$ and δ_{150} , $\delta_{150(2\text{ h})}$ respectively, represents short-time deformation. The stiffness for Type I pads is higher compared to Type II pads, although Type I pads are not further considered due to wear of the carbon ring [16]: while the central UHMWPE part is initially 2 mm above the carbon ring, visco-elastic deformation of the polyethylene surface (3.04 mm total vertical indentation) causes contact between the carbon ring and the convex counterface when loaded above 50 MPa, due to the counterface geometry. An additional polymer lip at the top surface is designed to flow plastically under

progressive loading between the carbon ring and the counterface, protecting against contact. The static deformation of pads with differences in lip geometries was experimentally tested and they have no uniform effect on the total vertical indentation and the stiffness, indicating good repeatability for determination of stiffness on full-scale specimen tests for lip diameters 244 and 239 mm. Lowering the lip diameter from 244 to 236 mm slightly lowers the indentation, however, it increases again for 237 mm lips. An important factor in this respect is the polyethylene flow at the onset of the lip contacting the carbon ring, which becomes restricted for lower lip diameter and/or thickness.

For a constant sample holder diameter (250 mm), the relation between initial pad diameter and deformation during loading at 150 MPa is illustrated in Table 1. Any variation on the nominal diameter is attributed to the manufacturing process of the hybrid pads.

Table 1
Vertical indentation under compressive load (short-time behaviour, 2 h) for a hybrid UHMWPE pad

| Pad type | Pad geometry (mm) Effective diameter | Lip geometry (mm) | | Vertical indentation and short-time deformation (mm) | | | | Stiffness (kN/mm) |
|----------|---|----------------------|-----------------------|--|---------------------------|----------------|---------------------------|-------------------|
| | | Nominal lip diameter | Nominal lip thickness | δ_{120} | $\delta_{120(2\text{h})}$ | δ_{150} | $\delta_{150(2\text{h})}$ | |
| Type I | 249.50 | No lip | | 2.80 | 2.82 | 3.04 | 3.07 | 6681 |
| | 249.50 | 236 | 1.6 | 2.16 | 2.24 | 2.52 | 2.62 | 5250 |
| | 249.50 | 244 | 1.1 | 3.54 | 3.62 | 3.98 | 4.10 | 4091 |
| | 249.50 | 244 | 1.5 | 3.22 | 3.28 | 3.68 | 3.73 | 3682 |
| Type II | 249.50 | 239 | 1.5 | 3.15 | 3.20 | 3.60 | 3.66 | 3682 |
| | 249.37 | 237 | 1.5 | 3.50 | 3.59 | 3.85 | 3.96 | 5665 |
| | 249.48 | 237 | 1.5 | 3.46 | 3.52 | 3.80 | 3.92 | 5260 |
| | 249.50 | 237 | 1.5 | 3.42 | 3.48 | 3.78 | 3.89 | 4910 |
| | 249.55 | 237 | 1.5 | 3.31 | 3.40 | 3.67 | 3.80 | 5455 |

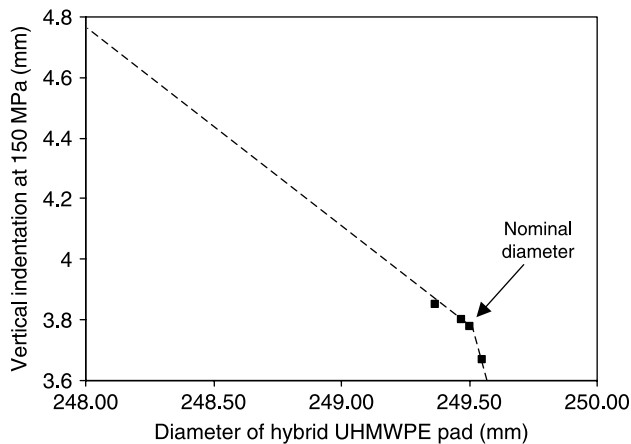


Fig. 5. Effect of variation in initial diameter of the hybrid UHMWPE pad on vertical deformation.

Ranging between 249.37 and 249.55 mm, a typical variation of less than 0.1% on the nominal diameter is achieved from moulding. For a hybrid UHMWPE pad with identical lip geometry and identical carbon fibre/epoxy reinforcing ring, the lower pad diameters result in progressive higher vertical indentation. From Fig. 5, it reveals that there is a bi-linear correlation between the effective pad diameter and the vertical indentation: oversized pad diameters have a strong reduction in vertical indentation, while undersized pad diameters slightly increase the vertical indentation. This indicates that the vertical deformation depends either on friction with the bottom of the sample holder (undersize), or on retaining by plastic deformation (oversize). In extremis, it is experimentally verified on a pad with diameter 248 mm, that there is an additional indentation of 1 mm (2.5%) during loading in correspondence to extrapolation in Fig. 5.

3.2. Creep

Experimental creep data is shown in Fig. 6. Short-time creep (2 h) for Type I and Type II pads is presented in Table 1. Results from both long-time creep tests (150 MPa, 24 h) and life-time creep tests (75 MPa, 7 days) are summarized in Table 2.

3.2.1. Long-time creep

Comparing the long-time creep deformation (Table 2) to short-time creep deformation (Table 1) reveals that most of the dimensional variation is established after 2 hours constant loading. For a Type I pad, creep at 150 MPa is only 0.03 mm (2 h) or 0.05 mm (24 h) as the deformation of UHMWPE is totally stabilised by the reinforcing carbon fibre/epoxy ring. It was already observed from the stress–strain characteristics that the UHMWPE is visco-elastically deformed under 150 MPa and any further deformation is restricted after the initial clearance between the hybrid UHMWPE pad and sample holder diameters has disappeared. The creep for Type II pads is larger than for Type I pads, mainly depending on the lip diameter and thickness. Contrasting to initial loading, variations in initial pad diameter between 249.55 and 249.37 mm for constant lip geometry have no unique influence on the creep behaviour. Considering a lip diameter of 244 mm causes high creep, 239 mm causes intermediate creep and 237 mm causes the lowest creep deformation. In combination with different lip thicknesses, lowering the thickness from 1.5 to 1.1 mm at constant diameter of 244 mm further decreases creep deformation. However, the combination between an optimum lip diameter and lip thickness is at 237 and 1.5 mm. Although the UHMWPE polymer lip did not

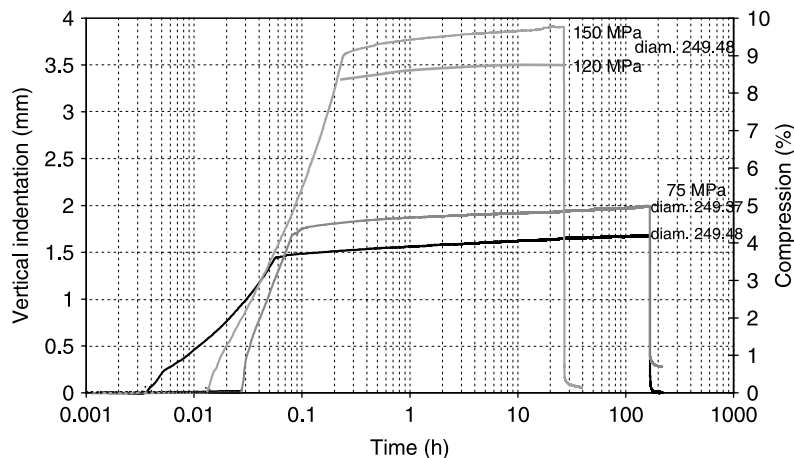


Fig. 6. Long-time and life-time creep (and 12 h recovery) for hybrid UHMWPE pads retained in a sample holder.

Table 2
Creep deformation (long-time behaviour, 24 h and life-time creep, 168 h) for a hybrid UHMWPE pad

| Pad type | Pad geometry (mm) | Lip geometry (mm) | | Long-time creep at 150 Mpa (mm) | Recovery (mm) | | Life-time creep 75 Mpa (mm) |
|----------|-------------------|----------------------|-----------------------|---------------------------------|---------------------|------|-----------------------------|
| | | Nominal lip diameter | Nominal lip thickness | | Immediate unloading | 12 h | |
| Type I | 249.50 | No lip | | 0.05 | 1.98 | 0.43 | – |
| | 249.50 | 236 | 1.6 | 0.19 | 2.10 | 0.38 | – |
| | 249.50 | 244 | 1.1 | 0.18 | 2.80 | 0.42 | – |
| | 249.50 | 244 | 1.5 | 0.32 | 3.25 | 0.68 | – |
| Type II | 249.50 | 239 | 1.5 | 0.20 | 2.65 | 0.54 | – |
| | 249.37 | 237 | 1.5 | 0.14 | 2.40 | 0.67 | 0.22 |
| | 249.48 | 237 | 1.5 | 0.15 | 2.45 | 0.76 | 0.23 |
| | 249.50 | 237 | 1.5 | 0.15 | 2.60 | 0.63 | – |
| | 249.55 | 237 | 1.5 | 0.16 | 2.58 | 0.54 | – |

affect the bulk properties and measured stiffness, it is important for the creep behaviour and protection of the carbon fibre/epoxy ring.

3.2.2. Life-time creep

The initial vertical indentation after application of the load is 1.77 mm or 1.47 mm depending on the initial diameter, while the additional creep of 0.22 mm is nearly identical for both pads. Again, the clearance between the pad and hole diameter determines the initial deformation in the elastic region, and once loaded above the yield strength further deformation is restricted by the sample holder and results in nearly identical creep. Then, the hybrid pad is completely retained and further creep is not influenced by differences in initial pad diameter. The lip diameter influences creep, as a very small difference in effective lip diameter (236.79 and 236.95 mm) results in higher creep deformation (0.22 and 0.23 mm) for the largest lip diameter.

3.3. Recovery and permanent deformation at zero stress

After creep deformation at 150 MPa, the stress was decreased to 30 MPa/min and recovery was further measured over 12 h (Fig. 6). The immediate recovery at unloading and recovery after 12 h under stress free conditions are listed in Table 2 for pads with different diameter and lip geometry. It seems that either after long-time or life-time creep the recovery is higher for pads with large initial diameter compared to small initial diameters, because the former were less plastically deformed under loading. From a design point of view, the permanent deformation of the hybrid polymer pad is more important, including a permanent change in total thickness, pad diameter and change in

lip diameter. High permanent thickness reduction leads to possible overload of a neighbouring polymer bearing element on the ball-joint, while high change in lip diameter causes curling and sliding instabilities with coating wear. The permanent thickness reduction of the hybrid pads is given in Table 3: in the centre of the pad it is calculated from on-line recovery measurements, compared to the permanent thickness reduction at the borders of the pad measured by a micrometer. Also, the permanent deformation in pad diameter at the bottom (not retained by the carbon fibre/epoxy ring) or lip diameter is measured by a micrometer.

The permanent deformation for a Type I pad in the centre is larger than at the borders due to the indentation of the curved counterface, as shown on a surface profilometer in Fig. 7a. For Type II pads, the deformation near the borders is either negative or positive due to stable or unstable deformation of the polymer lip (Fig. 7b). Although the initial clearance between the hybrid UHMWPE pad and the sample holder allows for deformation, the increase in diameter of the polyethylene part under plastic flow is very small as it is totally stabilised by the carbon fibre/epoxy ring. The permanent radial deformation of the carbon ring is between 0.07 and 0.17 mm, showing that it bears the deformation at 150 MPa with a combination of high radial and tangential stresses under hydrostatic conditions. For Type II pads, the increase in pad diameter is somewhat larger due to optimisation of the carbon fibre/epoxy ring geometry (for details see [16]) allowing for higher deformation. With a constant lip diameter of 237 mm, there is a clear trend that the higher the effective diameter, the lower the permanent increase in diameter due to the retaining action of the sample holder. As such, the final diameter of the UHMWPE hybrid pads after loading and recovery is

Table 3
Permanent deformation of a hybrid UHMWPE pad after long-time creep and life-time creep

| Pad type | Pad geometry (mm) Effective diameter | Lip geometry (mm) | | Thickness deformation ^a (mm) | | Diameter increase (mm) | |
|-------------------------|---|----------------------|-----------------------|---|---------|------------------------|--------------|
| | | Nominal lip diameter | Nominal lip thickness | Centre | Borders | Pad diameter | Lip diameter |
| Long-time creep (24 h) | | | | | | | |
| Type I | 249.50 | No lip | | - 0.68 | - 0.30 | 0.07 | No lip |
| | 249.50 | 236 | 1.6 | - 0.23 | - 0.18 | 0.43 | 3.78 |
| | 249.50 | 244 | 1.1 | - 0.94 | - 0.34 | 0.45 | 2.75 |
| | 249.50 | 244 | 1.5 | - 0.94 | + 1.42 | 0.40 | 3.39 |
| Type II | 249.50 | 239 | 1.5 | - 0.61 | - 0.42 | 0.41 | 3.70 |
| | 249.37 | 237 | 1.5 | - 0.92 | + 0.28 | 0.31 | 6.48 |
| | 249.48 | 237 | 1.5 | - 0.74 | + 0.25 | 0.23 | 5.74 |
| | 249.50 | 237 | 1.5 | - 0.70 | + 0.17 | 0.22 | 4.66 |
| | 249.55 | 237 | 1.5 | - 0.71 | + 0.21 | 0.14 | 6.23 |
| Life-time creep (168 h) | | | | | | | |
| Type II | 249.37 | 237 | 1.5 | - 0.11 | + 1.56 | 0.14 | 4.01 |
| | 249.48 | 237 | 1.5 | - 0.27 | + 0.62 | 0.05 | 3.36 |

^a Negative value is permanent indentation, positive value is permanent increase in thickness compared to 40 mm original, due to irregular lip formation.

between 249.68 and 249.72 mm allowing for total fixation in the sample holder.

For Type II pads the permanent increase in lip diameter depends on the initial lip geometry, both its

diameter and thickness. For a 244 mm lip and thickness between 1.1 and 1.5 mm, there is an increase of 2.75 mm (1.12%) or 3.39 mm (1.39%): a higher lip thickness allows for more extrusion of the polyethylene

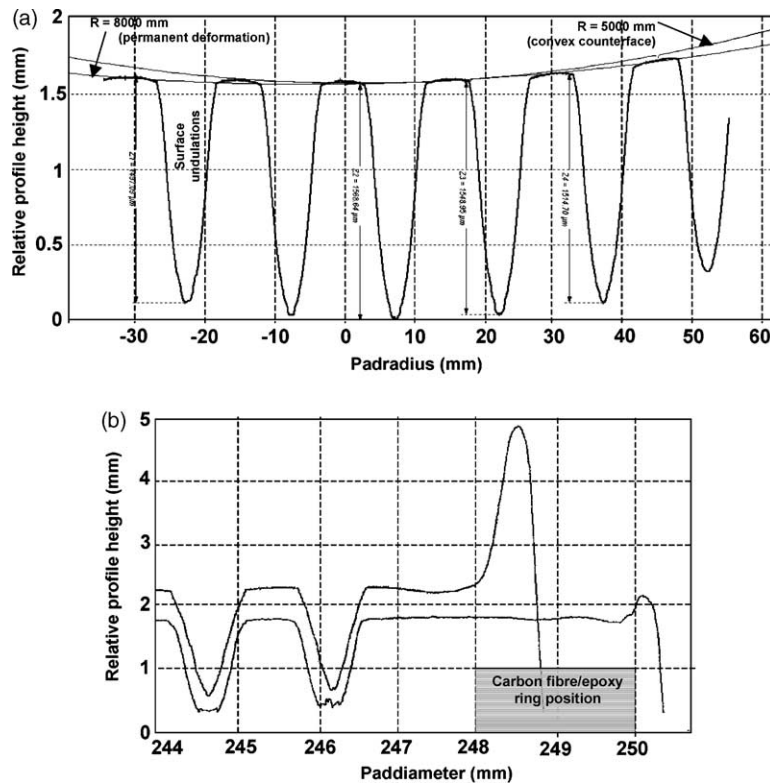


Fig. 7. Surface profile, representing permanent deformation of a hybrid UHMWPE pad after loading at 150 MPa and recovery, (a) Centre of the polymer pad with permanent indentation of convex counterface, (b) Borders of the polymer pad with regular and irregular lip deformation.

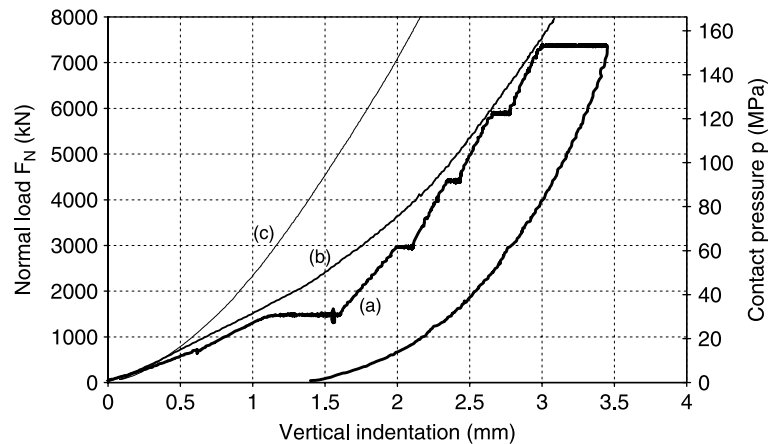


Fig. 8. Stress–strain characteristics of a hybrid UHMWPE pad during multiple loading steps, (a) first loading step, (b) second loading step not retained, (c) second loading step retained.

between the carbon ring and the convex counterface with better protection. In combination with a 244 mm diameter, however, irregular deformation of the lip with 1.5 mm thickness is reflected by a high increase in thickness at the borders (+1.42 mm), indicative of curled lips. Therefore, different combinations of lip diameter and thickness were investigated with an average increase of 3.39 mm for a 244 mm lip (1.39%), 3.70 for a 239 mm lip (1.54%), 4.41 mm for a 237 mm lip (1.86%) and 3.78 mm for a 236 mm lip (1.60%). There is a tendency that small initial lip diameters show the highest deformation, with an optimum at 237 mm initial diameter, due to effective deformation and cold flow between the carbon ring and the convex counterface. Lower lip diameters of 236 mm do not cover the carbon ring effectively, although a thickness of 1.6 mm was applied providing higher resistance to cold flow. According to Engh et al. [17], as observed on small-scale test samples, the cold flow of UHMWPE refers to a surface phenomenon that is due to deformation of a material under the influence of shear forces in absence of elevated temperatures. For the optimised lip geometry (237 mm × 1.5 mm), the total lip deformation depends also on the initial pad diameter: the most stable deformation is obtained on a pad with 249.50 mm effective diameter, and either oversized (249.55 mm) or undersized (249.37–249.48 mm) pad diameters results in higher lip deformation and curling due to different distribution of the creep deformation between bulk and surface. After life-time creep, the recovery and permanent lip deformation is less stable, as concluded from the increase of over 1.56 mm at the borders of the pads.

3.4. Influence of multiple creep and subsequent loading

After loading and unloading the hybrid UHMWPE pad at normal working conditions of 150 MPa, a second loading step was applied at 30 MPa/min without stepwise control at intermediate stress levels, following the stress–strain characteristics as shown in Fig. 8. A test is done either with free expansion of UHMWPE at the bottom of the sample holder or totally retained by the sample holder and reinforcing ring:

- Under free expansion, differences in vertical indentation are mainly concentrated at low load levels (30–60 MPa), where the vertical indentation for a given normal load during the second loading step is lower compared to the first loading step. Moreover, a linear relationship with higher modulus is measured over 1.4 mm vertical indentation, while linearity only occurred over 0.4 mm vertical indentation during the first loading step. The loading region with a linear characteristic corresponds to the zone where creep was allowed during initial loading. Under high load levels (120–150 MPa), there is good coincidence between the total vertical indentation from direct loading and accumulated creep in the first and second loading histories.
- When totally retained by the sample holder and the carbon reinforcing ring, the initial linear elastic deformation zone has disappeared, resulting in lower total indentation. Creep during the initial loading step is now favourable for reduction of the clearance between the pad diameter and the sample holder diameter, reducing the effects of initial pad diameter on the deformation behaviour.

3.5. Failure at overload

Overload conditions were applied on a Type II hybrid UHMWPE pad under 180 MPa. The maximum load was applied at 30 MPa/min during a second loading step, immediately rising to the maximum load. The vertical indentation and stiffness in the 150–180 MPa load range are given in Fig. 9a and Table 4, compared to the deformation in the first loading step. In the 150–180 MPa load range, the variation of stiffness and total vertical indentation is lower compared to the stress–strain characteristics measured in Fig. 4, and the total vertical indentation varies between 2.64 and 2.90 mm. Also, polymer pads showing excess deformation under initial loading at 150 MPa, have lower deformation during re-loading at 180 MPa. The initial pad diameter seems, however, to influence the vertical indentation in the opposite way compared to the first loading step, with higher deformation as the initial diameter is increased. This behaviour is in accord with the differences in immediate recovery measured in Table 2. The measurements at overload reflect the influence of degradation under creep and recovery, as higher deformation and recovery during the first loading step corresponds to lower deformation during

the second loading step. Corresponding to previously described dependencies between visco-elastic deformation and vertical indentation, there is a small decrease in stiffness from 4910 kN/mm² (initial loading at 150 MPa) to 4745 N/mm² (loading at 180 MPa), while the variation in stiffness becomes smaller.

Failure at overload under 200 and 400 MPa is simulated on a hybrid pad with diameter 175 mm owing to the limited capacity of the hydraulic test bench. The characteristic stress–strain curve for a Type I hybrid UHMWPE pad is shown in Fig. 9b. Maintaining the normal load constant at 200 MPa for 2 h yields very high creep (1 mm) compared to 150 MPa (0.03 mm). With an immediate recovery of 4.1 mm during unloading from 400 MPa and a 0.56 mm recovery during 12 h under stress-free conditions, there remains a permanent indentation of the hybrid UHMWPE pad of 1.5 mm. Although its local integrity and functionality as a load bearing element is not affected after an overload, replacement in the ball joint is advised through loss of contact with the convex counterfaces relative to its neighbouring elements. As the diameter to thickness ratio of 175 mm pad is different than for full-scale tests, that geometry is not representative for calculating the stiffness and is only used to demonstrate a loading capacity of 400 MPa.

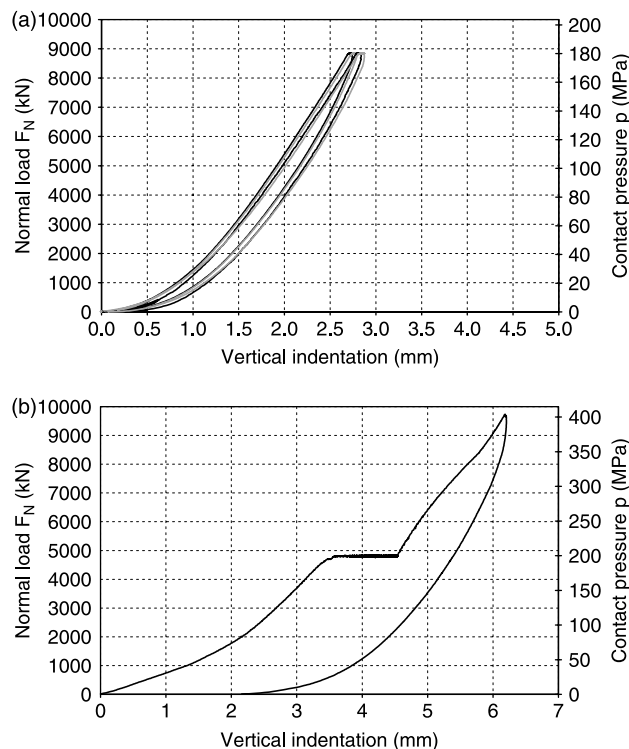


Fig. 9. Stress–strain characteristics for hybrid UHMWPE pads under overload conditions to (a) 180 MPa, (b) 200, 400 MPa.

Table 4
Overload deformation of a hybrid UHMWPE pad

| Pad type | Pad geometry (mm) | | Lip geometry (mm) | | Vertical indentation (mm) | | | | Stiffness (kN/mm) |
|----------|--------------------|----------------------|-----------------------|----------------|---------------------------|----------------|----------------|----------------|--------------------|
| | Effective diameter | Nominal lip diameter | Nominal lip thickness | First loading | | Second loading | | | |
| | | | | δ_{150} | δ_{150} | δ_{180} | δ_{200} | δ_{400} | |
| Type I | 249.50 | No lip | | 3.04 | 2.61 | 2.86 | 3.03 | – | Not representative |
| Type II | 175.00 | No lip | | 2.99 | 2.93 | 3.10 | 3.57 | 6.15 | |
| | 249.37 | 237 | 1.5 | 3.85 | 2.34 | 2.64 | – | – | 4903 |
| | 249.48 | 237 | 1.5 | 3.80 | 2.43 | 2.79 | – | – | 4903 |
| | 249.50 | 237 | 1.5 | 3.78 | 2.53 | 2.84 | – | – | 4745 |
| | 249.55 | 237 | 1.5 | 3.67 | 2.58 | 2.90 | – | – | 4596 |

3.6. Statistical analysis of large-scale specimen tests

Validation tests on hybrid UHMWPE pads were performed for statistical analysis of large-scale specimen tests and quality control of the production process of the hybrid pads. From failure analysis of the entire construction, it is concluded that a series of three tests on each production batch of hybrid UHMWPE pads provides good reproducibility. More tests increase the accuracy of the test result, however it is not relevant for the real ball-joint construction due to discrepancies between laboratory tests and the real construction, mainly considering edge effects. Safety factors will compensate for experimental uncertainties. For Type II hybrid pads with nominal lip diameter 237 mm, nominal lip thickness 1.5 mm and effective diameter 249.37 mm, Table 5 shows the variation in vertical indentation at 120, 150 MPa, the creep for 24 h at 150 MPa, vertical indentation at overload of 180 MPa, and the recovery under 24 h stress free conditions. The average and standard deviation is calculated and will be used for

further implementation and modelling of the deformation of a prototype hybrid UHMWPE pad. Values from large-scale deformation and creep tests seem in good (2.2%) to very good (0.4%) agreement. The recovery behaviour is less reproducible (standard deviation 6.4%), as it depends strongly on any variation in the previous loading history. For the first loading step at 120 and 150 MPa, reproducibility decreases with increasing normal load, although during the second loading step at 180 MPa, the reproducibility improves. Creep is the most reproducible. Due to the previously explained influence of visco-elastic deformation, the importance of the initial clearance between polymer pads and sample holders disappears at higher contact pressures and the reproducibility becomes less dependent on the manufacturing process under progressively higher normal loads.

3.7. Visual evaluation of contact surfaces

Macroscopic photographs of the hybrid UHMWPE pad with initial lip diameter 237 mm after loading

Table 5
Statistical analysis of large-scale compression tests

| Pad type | Pad geometry (mm) | | Lip geometry (mm) | | Vertical indentation (mm) | | | | Stiffness (kN/mm) |
|------------------------|--------------------|----------------------|-----------------------|----------------|---------------------------|-------|----------------|----------|-------------------|
| | Effective diameter | Nominal lip diameter | Nominal lip thickness | δ_{120} | δ_{150} | Creep | δ_{180} | Recovery | |
| Type II | 249.37 | 237 | 1.5 | 3.52 | 3.89 | 0.13 | 2.64 | 0.57 | 5665 |
| | 249.37 | 237 | 1.5 | 3.51 | 3.82 | 0.14 | 2.60 | 0.67 | 5892 |
| | 249.37 | 237 | 1.5 | 3.49 | 3.85 | 0.14 | 2.66 | 0.76 | 5438 |
| Average (mm) | | | | 3.50 | 3.85 | 0.14 | 2.64 | 0.67 | 5665 |
| Standard deviation (%) | | | | 1.1 | 2.4 | 0.4 | 2.2 | 6.4 | 1.5 |

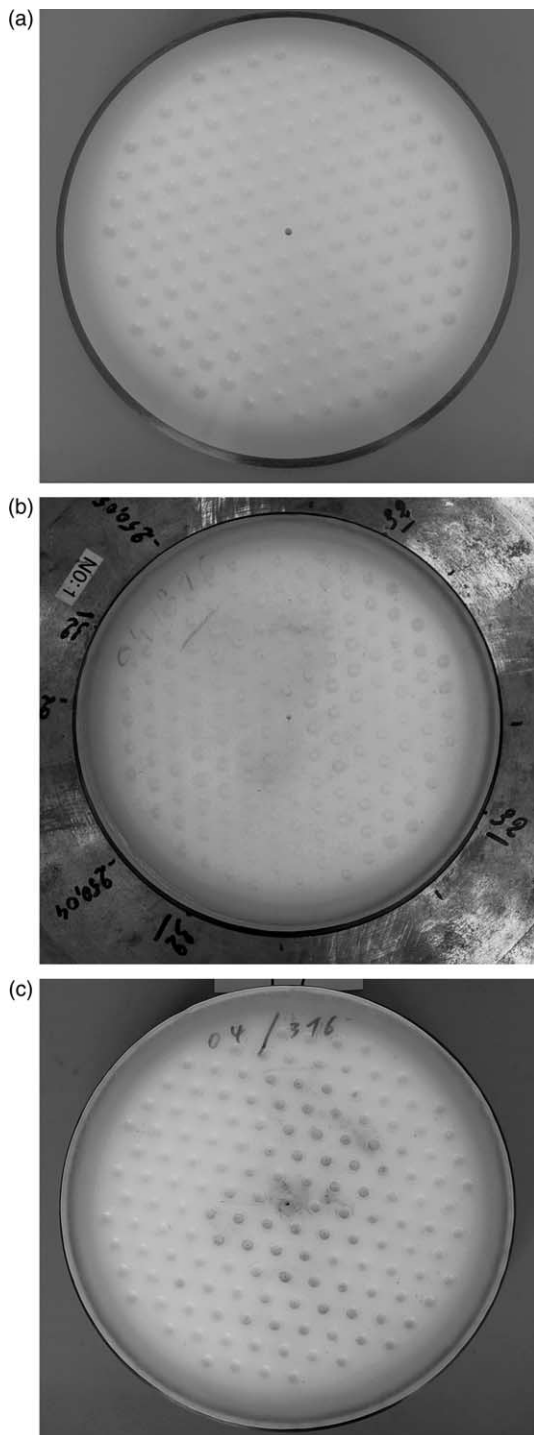


Fig. 10. Macroscopic photograph of a hybrid UHMWPE pads (pad diameter 249.50 mm, lip diameter 237 mm, lip thickness 1.5 mm) after compressive loading at (a) 30 MPa, (b) 150 MPa, (c) 180 MPa.

against a Zn-phosphate coating at 30, 150 and 180 MPa (with recovery) are shown in Fig. 10. The lip diameter has hardly increased after loading at 30 MPa and

therefore it does not adequately cover the carbon fibre/epoxy ring. Under low loads, full protection against contact with the Zn-coated counterface is, however, not required: due to the convex geometry of the counterface, there is no contact between the coating and the carbon ring, and mainly the centre of the ball is indented. Under 150 MPa normal load, there is contact over the full bearing area of the polymer pad and protection is required. Now the polymer lip has regularly flowed over the entire carbon ring. After loading at 180 MPa, the polymer lip wraps the carbon fibre/epoxy ring totally and has some tendency for curling. The latter mainly occurs after removal of the normal load, as internal stresses accumulate in the lip under elastic recovery ('shrinkage-effect'). While the polymer lip was loaded, it remained flat between the convex surface and the carbon ring, not causing sliding instabilities. Unstable curling of a 244 mm lip is illustrated in side-view in Fig. 11a. Also, after life-time creep under 75 MPa, the lip deformation was rather unstable compared to long-time creep after 150 MPa. Confirmed by the large increase in thickness in Table 3 or Fig. 7b, the cross-sectional view in Fig. 11b shows that the lip is free from the carbon fibre/epoxy ring and possibly damages the primer coating. These phenomena are attributed to low contact pressures and limited cold flow of the polymer lip. A cross-sectional view in Fig. 11c shows good contact between the polymer lip and the carbon ring after loading to 150 MPa, while no failure of the carbon fibre/epoxy ring was observed. However, experience has shown that the composition and production parameters of the composite ring should be held within narrow tolerances as they strongly influence the strength of the reinforcing ring. Separate selection tests for the carbon fibre/epoxy ring were developed in Ref. [18]. Near the bottom of the hybrid UHMWPE pad, the circumferential groove and rubber ring have not deformed and function well for fixation in the sample holder. Both after long-time creep at 150 MPa and life-time creep at 75 MPa, there was no relaxation of the rubber O-ring observed, it remained pre-stressed with good restraining characteristics.

The Zn-phosphate primer on the convex counterface after static loads of 180 MPa is shown in Fig. 12, exhibiting either good stability or wear depending on the curing time of the coating and stability of the polymer lip. After only 4 days curing time, the coating is worn in the contact zones with the polymer lip and bare steel is exposed. With one week curing time, the adhesion between coating and steel is improved and, although some deformation of the coating is observed in case of irregular lip deformation, it is not detrimental

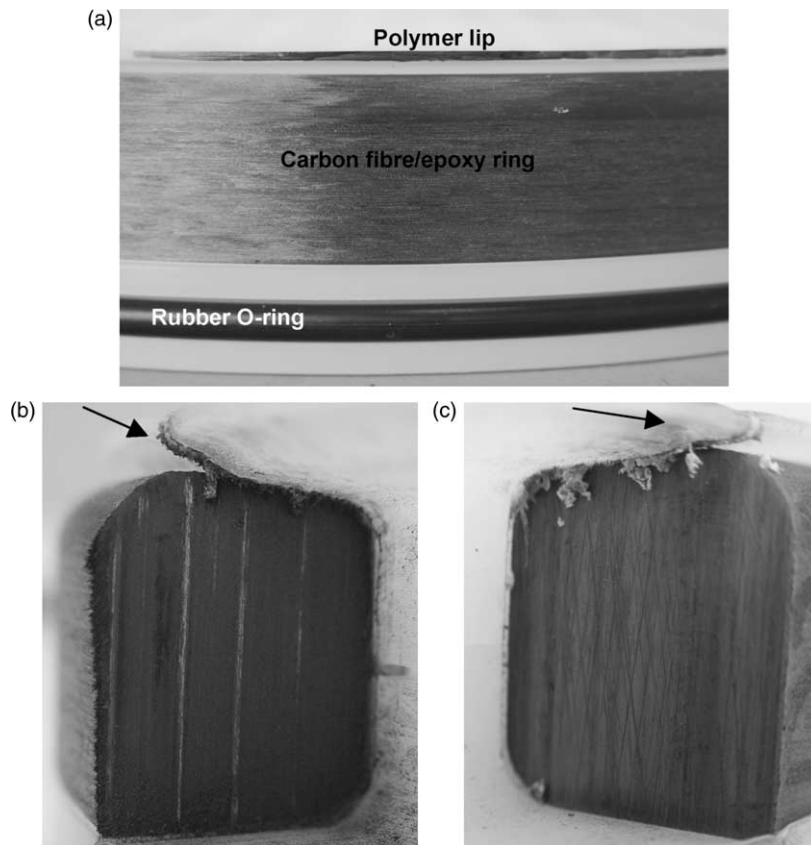


Fig. 11. Details of the polymer lip deformation and groove for rubber O-ring after loading at 180 MPa and recovery, (a) side-view with unstable lip deformation (life-time creep), (b) cross-sectional view with unstable lip deformation: curling (lip diameter 244 mm), (c) cross-sectional view with stable lip deformation: flat (lip diameter 237 mm).

to the prevention of corrosion of the steel surface. There is a small indentation of the lubricating holes of the pad in the centre of the counterface and slip marks are observed in contact with the polymer lip. The latter points towards friction between the coating and the polymer lip due to relative motion under extrusion of the polymer lip. The good wear resistance and low friction of the coating was, however, demonstrated by large-scale sliding tests [7]. In the case of unstable lip formation, deeper grooves and flakes are observed that do not affect the wear resistance, but contribute to higher sliding resistance under subsequent closure actions of the ball joint. The effect of mutual adhesion under creep between the UHMWPE surface and the coating on subsequent sliding was, therefore, investigated and reported in Ref. [7]. In parallel to the friction and wear tests, indentation of the polymer lip without fracture of the Zn-phosphate primer coating points towards visco-elastic behaviour of the coating with self-repairing capability. From both static and dynamic testing of the coating, the average coating thickness in

wet conditions is optimised at 175 and 40 to 80 μm in dry conditions (drying time 1 h, curing time 1 week). Attention should be paid to the application procedures (brushing, spraying or rolling) as they influence the sliding and wear behaviour.

4. Discussion

It is demonstrated that the compressive strength of a hybrid UHMWPE-pad/Zn-phosphate coating is high and large-scale test results obtained on different pad geometries are reproducible. For a successful design of the entire ball-joint and steel structures, however, two small details of the hybrid UHMWPE pads are experimentally verified to have crucial importance:

- Besides the visco-elastic properties of the UHMWPE type GUR 4120, the local stiffness and total vertical indentation of a pad is determined by its geometry and the tolerances of the pad diameter and sample holder.

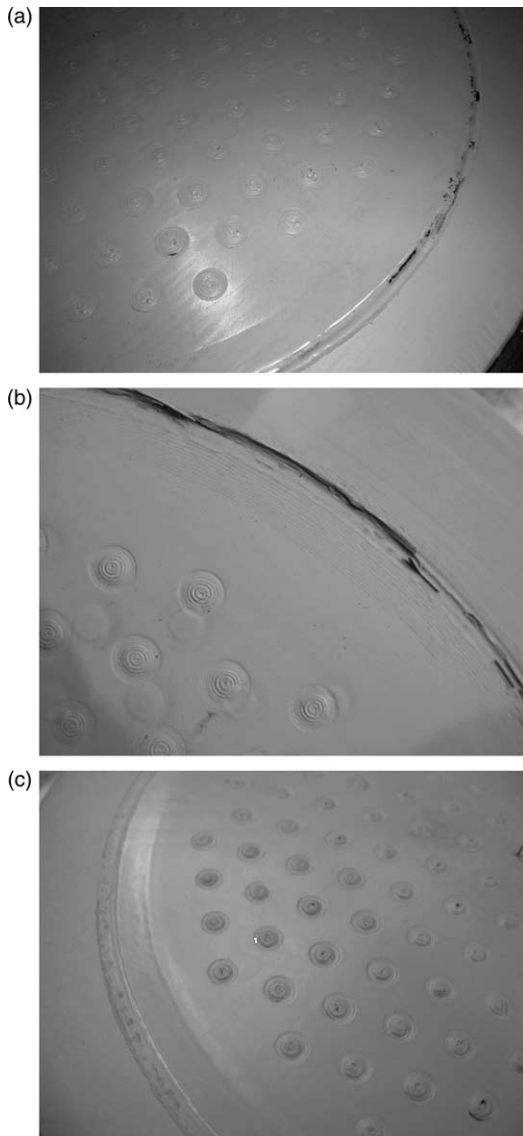


Fig. 12. Zn-phosphate primer coating on the convex counterface after loading at 180 MPa, (a) wear after 4 days curing time, (b) wear after 7 days curing time with irregular polymer lip deformation, (c) good corrosive protection after 7 days curing time and favourable polymer lip deformation.

- For protecting extrusion of the polymer lip between the carbon fibre/epoxy reinforcing ring and the Zn-phosphate primer coated counterface and stable deformation after creep and recovery, the polymer lip thickness and lip diameter should be carefully chosen.

The retaining action of the sample holder on the deformation of the UHMWPE pad is illustrated Fig. 13. The initial Young's modulus is calculated to be

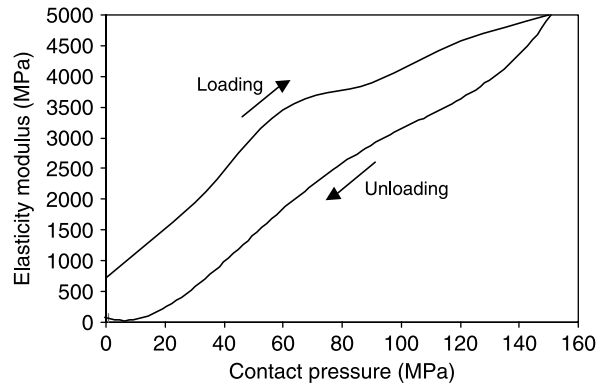


Fig. 13. Evolution of elasticity modulus with increasing contact pressure (vertical indentation) due to the retaining action of the sample holder.

between 710 and 720 MPa, corresponding to a modulus of 720 MPa from a standard tensile stress–strain curve. At deformation under high loads, however, there is a progressive increase in modulus, finally attaining 4910 MPa under 150 MPa. The difference between elasticity moduli during the loading and unloading steps are attributed to hysteresis effects. For the present test geometry, free visco-elastic deformation of the hybrid UHMWPE pad is initially allowed through the clearance in diameter between pad and specimen holder. However, radial deformation is restricted by the reinforcing carbon fibre/epoxy ring and deformation at the bottom is restricted by friction, resulting in a non-linear stress–strain characteristic. Stresses by normal loading of the hybrid pad are initially transferred into the steel structure only through the bottom of the sample holder. Once above 60 to 80 MPa, an increase in slope of the stress–strain curve is noticed, while the dependency of calculated stiffness on diameter tolerances decreases. Loaded above its yield strength, the initial clearance on the pad and sample holder diameter has disappeared by creep deformation of the polymer pad. The plastic flow of UHMWPE is now retained by the sample holder and stresses are additionally conducted into the steel walls of the sample holder. Then, the hybrid pad behaves under hydrostatic conditions. As the static deformation of the hybrid UHMWPE pad depends strongly on the retaining action of the specimen holder, the dimensions of both hybrid pads and sample holders should be subject to narrow tolerances for practical application and uniform distribution of the contact stresses.

From variations in lip geometry and bulk diameter, it seems that the loading characteristic and stiffness of a hybrid pad under yielding conditions is mostly

determined by its bulk properties (dimensions and modulus) rather than the surface properties (lip geometry), while retained in a sample holder. Creep and recovery deformation depends on good design of the lip thickness and lip diameter, yielding protective cold flow and avoiding lip curls. The latter mainly depends on stress relaxation during recovery and is indirectly controlled by the deformation under loading, where cold flow of the polymer lip on the top surface progressively increases with loading time. The viscoelastic material flow under yielding conditions is however controlled by the geometry between the carbon ring and the ball counterface, where excess material (large lip diameter and large lip thickness) results in high creep deformation and little material (low lip diameter and low lip thickness) results in failure. An optimum geometry is experimentally determined, and will be mathematically modelled in the second part of this creep design study.

5. Conclusions

Experimental results from static compression tests are discussed in relation to the geometry of the UHMWPE hybrid pad, in order to understand the deformation behaviour of the polymer disc under 150 MPa and the influence of a retaining steel wall (sample holder). For a homogeneous deformation, the pad diameters should have narrow tolerances and the lip geometry should be carefully selected. For the latter, instabilities are attributed to curling after extrusion of polyethylene between the carbon ring and the convex counterface, and recovery. An optimum lip geometry was therefore experimentally selected. The stiffness results from a combination of intrinsic compressive modulus of the polymer pad, the pad diameter, the pad thickness, the diameter and the depth of the sample holder. The local behaviour of a single polymer pad will be further modelled and can now be connected to the entire ball-joint construction, where the UHMWPE pads function as sliding material.

Acknowledgements

The authors express their gratitude to Solico B.V. and the Ministry of Transport, Public Works and Water Management (The Netherlands), allowing to present the test results and to be involved in the redesign of the Maeslant storm surge barrier.

References

- [1] P. Samyn, P. De Baets, Friction of polyoxymethylene homopolymer in highly loaded applications extrapolated from small-scale testing, *Tribol. Lett.* 19 (2005) 177–189.
- [2] O. Colak, Modeling deformation of polymers with viscoplasticity theory based on overstress, *Int. J. Plasticity* 21 (2005) 145–160.
- [3] J. Raghavan, M. Meshii, Creep of polymer composites, *Compos. Sci. Technol.* 57 (1997) 1673–1688.
- [4] S.F. Zheng, G.J. Weng, A new constitutive eq. for the long-term creep of polymers based on physical aging, *Eur. J. Mech. A21* (2002) 411–421.
- [5] J.V. Suvorova, N.G. Ohlson, S.I. Alexeeva, An approach to the description of time-dependent materials, *Mater. Des.* 24 (2003) 293–297.
- [6] D.W. Scott, A.H. Zureick, Compression creep of a pultruded E-glass vinylester composite, *Compos. Sci. Technol.* 58 (1998) 1361–1369.
- [7] P. Samyn, L. Van Schepdael, J.S. Leendertz, A. Gerber, W. Van Paepegem, P. De Baets, J. Degrieck, Large-scale friction and wear tests on a hybrid UHMWPE-pad/primer coating combination used as bearing element in an extremely high-loaded ball-joint, *Trib. Int.*, in press.
- [8] J.P. Collier, M.B. Mayor, J.L. McNamara, Analysis of the failure of 122 polyethylene inserts from uncemented tibial knee components, *Clin. Orthop. Relat. Res.* 273 (1991) 232–242.
- [9] F.F. Buechel, M.J. Pappas, G. Makris, Evaluation of contact stress in metal-backed patellar replacements, *Clin. Orthop. Relat. Res.* 273 (1991) 190–197.
- [10] D.L. Bartel, V.L. Bicknell, T.M. Wright, The effect of conformity, thickness and material on stresses in UHMWPE, components, *J. Bone Joint Surg.* 68 (1986) 1041–1051.
- [11] W.C. Hayes, V.K. Lathi, T.Y. Takeuchi, Patello-femoral contact pressures exceed the compressive yield strength of UHMWPE, *Trans. 39th ORS*, 1993, p. 421.
- [12] R.E. Bristol, D.C. Fitzpatrick, T.D. Brown, J.J. Callaghan, Non-uniformity of contact stress on polyethylene inserts in total knee arthroplasty, *Clin. Biomech.* 11 (1996) 75–80.
- [13] R.W. Hood, T.M. Wright, T. Fukubayashi, A.H. Burstein, Contact area distribution in total knee replacements, *Trans. 27th ORS*, 1981, p. 181.
- [14] Ticona GmbH, Ultra high molecular weight polyethylene: product catalogue GUR, 2002, pp. 4–7.
- [15] S.M. Kurtz, L. Pruitt, C.W. Jewett, R.P. Crawford, D.J. Crane, A.A. Edidin, The yielding, plastic flow and fracture of UHMWPE used in total joint replacements, *Biomaterials* 19 (1998) 1989–2003.
- [16] P. Samyn, P. De Baets, W. Van Paepegem, L. Van Schepdael, E. Suister, J.S. Leendertz, Design of a carbon/epoxy reinforcing ring reducing creep of UHMWPE in high-loaded sliding contacts, 8th International Conference on Tribology, Veszprem, 2004, pp. 89–96.
- [17] G.A. Engh, K.A. Dwyer, C.K. Hanes, Polyethylene wear of metal-backed tibial components in total and unicompartmental knee prosthesis, *J. Bone Joint Surg.* 74B (1) (1992) 9–17.
- [18] W. Van Paepegem, L. Van Schepdael, J. Degrieck, P. Samyn, P. De Baets, E. Suister, J.S. Leendertz, Fast characterization of carbon/epoxy rings for use in the ball-joints of the Maeslant storm surge barrier. *Compos. Struct.*, in press.